

NMR Methods

A Simple Route to Strong Carbon-13 NMR Signals Detectable for Several Minutes

Soumya S. Roy,^[a] Philip Norcott,^[a] Peter J. Rayner,^[a] Gary G. R. Green,^[b] and Simon B. Duckett^{*[a]}

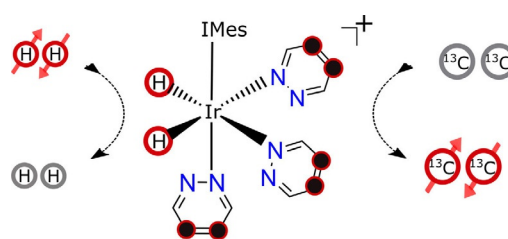
Abstract: Nuclear magnetic resonance (NMR) and magnetic resonance imaging (MRI) suffer from low sensitivity and limited nuclear spin memory lifetimes. Although hyperpolarization techniques increase sensitivity, there is also a desire to increase relaxation times to expand the range of applications addressable by these methods. Here, we demonstrate a route to create hyperpolarized magnetization in ¹³C nuclear spin pairs that last much longer than normal lifetimes by storage in a singlet state. By combining molecular design and low-field storage with *para*-hydrogen derived hyperpolarization, we achieve more than three orders of signal amplification relative to equilibrium Zeeman polarization and an order of magnitude extension in state lifetime. These studies use a range of specifically synthesized pyridazine derivatives and dimethyl *p*-tolyl phenyl pyridazine is the most successful, achieving a lifetime of about 190 s in low-field, which leads to a ¹³C-signal that is visible for 10 minutes.

Although carbon is one of the most abundant elements in nature, its NMR-active form carbon-13 is present at only about a 1.1% level which, when coupled with its low magnetogyric ratio, results in low detectability. Consequently, ¹³C magnetic resonance imaging (MRI) produces a negligible response when compared to proton measurement in the body, which is facile due to high water content and high sensitivity. ¹³C detection does, however, benefit from potentially long relaxation times when compared to those of the proton.

A number of methods, commonly known as hyperpolarization, exist that can increase NMR sensitivity in nuclei such as ¹³C and are being used to overcome these issues.^[1,2] These ap-

proaches artificially increase the associated spin population differences between the energy levels that are probed. For example, Golman et al. reported a *para*-hydrogen (*p*-H₂) induced nuclear polarization (PHIP) study,^[3,4] which achieved the rapid in vivo detection of a ¹³C-MRI response in 2001.^[5] Two years later, they described the results of a similar study using dissolution dynamic nuclear polarization (DNP),^[6] in which a normally inaccessible response was seen in vivo. Bhattacharya et al. have since incorporated *p*-H₂ into sodium 1-¹³C acetylene dicarboxylate to facilitate the collection of an arterial ¹³C-MRI image of a rat brain.^[7] More recently, a DNP-derived ¹³C-MRI response with chemical shift resolution has been shown to distinguish different metabolic flux between normal and tumor cells in humans.^[8–11] These studies illustrate the potential benefits to human health if such methods were to become widely accessible and hence establish the need for a rapid and low-cost delivery method for long-lived ¹³C hyperpolarization.

In this article, we demonstrate that the goal of rapidly producing a long-lived ¹³C hyperpolarized response can be met by applying the signal amplification by reversible exchange (SABRE) effect.^[12–14] In SABRE, a catalyst reversibly binds *p*-H₂ and the substrate to transfer dormant spin order from *p*-H₂ into the substrate through the scalar-coupling framework, as shown in Scheme 1. We use this approach here to hyperpolarize a series of coupled ¹³C spin-pairs in a range of pyridazine derivatives, a motif that exhibits pharmacological activity.^[15–16]



Scheme 1. Schematic depiction of the SABRE hyperpolarization technique. IMes = 1,3-bis(2,4,6-trimethylphenyl)imidazol-2-ylidene.

Polarization is then stored in specially created singlet spin order to enable a response to be seen several minutes later. Although a range of nicotinamide- and pyridazine-based substrates have been shown to deliver long-lived ¹H hyperpolarization,^[17,18] and analogous ¹⁵N-based singlets have been created by Warren and co-workers,^[19] we believe the ¹³C responses

[a] Dr. S. S. Roy, Dr. P. Norcott, Dr. P. J. Rayner, Prof. Dr. S. B. Duckett
Department of Chemistry, University of York
Heslington, York, YO10 5DD (UK)
E-mail: simon.duckett@york.ac.uk

[b] Prof. Dr. G. G. R. Green
York Neuroimaging Centre
The Biocentre, York Science Park Innovation Way, Heslington
York, YO10 5NY (UK)

Supporting information and the ORCID number(s) for the author(s) of this article can be found under <https://doi.org/10.1002/chem.201702767>.

© 2017 The Authors. Published by Wiley-VCH Verlag GmbH & Co. KGaA. This is an open access article under the terms of the Creative Commons Attribution License, which permits use, distribution and reproduction in any medium, provided the original work is properly cited.

reported here are significant due to the growing use of ^{13}C -MRI for in vivo study.

The term singlet ($|S_0\rangle = (|\alpha\beta\rangle - |\beta\alpha\rangle)/\sqrt{2}$) that is used here represents the spin-zero magnetic alignment of a coupled spin-1/2 system, the conversion of which into the associated triplet states ($|T_0\rangle = (|\alpha\beta\rangle + |\beta\alpha\rangle)/\sqrt{2}$; $|T_1\rangle = |\alpha\alpha\rangle$; $|T_{-1}\rangle = |\beta\beta\rangle$) is symmetry-forbidden. Consequently, any population difference that can be created between these singlet and triplet forms is expected to relax more slowly than the usual time constant T_1 .^[20] The symmetry properties that make such states long-lived also make them challenging to generate and probe.^[20,21] Levitt and co-workers have demonstrated a number of strategies to do this in a range of chemically inequivalent spin systems^[22–26] and have achieved a lifetime of over one hour in an optimized chemical system at low field.^[27] However, when a substantial chemical shift difference exists between these spin-pairs, the application of a spin-lock, or sample-shuttling to low field, is necessary to extend state lifetime.^[22,28,29] This effect has recently been illustrated by monitoring the effect of solvent-dependent chemical-shift changes.^[17,18] Warren and co-workers have reported a parallel approach that exploits magnetic inequivalence to create related singlet states.^[21,30–33] Thus, whereas SABRE has been shown to create hyperpolarized ^1H - and ^{15}N -derived singlets, there is a need to expand these methods to ^{13}C given the success of DNP.^[8–11] However, ^{13}C -SABRE itself has currently seen limited application^[34] and reported efficiency gains are relatively low. We have now developed a molecular design strategy for use with SABRE and radio frequency (*rf*) excitation to achieve greater than 2% net ^{13}C polarization in a long-lived form.

In this study, we employ magnetic and chemical inequivalence effects through the synthesis of specific substrates in which their carbon-4 and carbon-5 sites are ^{13}C -enriched, as detailed in Scheme 2 (full synthetic strategy and characteriza-



Scheme 2. The molecular systems studied here are of *Type-1*, which reflect a chemically equivalent but magnetically distinct ^{13}C spin-pair (black and red dots), or *Type-2a* and *Type-2b*, which reflect chemically inequivalent ^{13}C spin-pairs ($R^1 \neq R^2 \neq R^3$).

tion data are available in the Supporting Information, Section S1–3). The *Type-1* form agents exhibit chemically equivalent but magnetically inequivalent ^{13}C spin-pairs ($\Delta\delta = 0$) and have local C_2 symmetry. The *Type-2a* form is constructed such that R^1 and R^2 are chemically different and a small chemical-shift difference results between the ^{13}C spin-pair ($\Delta\delta \neq 0$). Chemical inequivalence is also derived by remote substitution at R^2 and R^3 , in the *Type-2b* agents of Scheme 2. Although these synthetic strategies allow access to two distinct classes of molecular system, our results illustrate that both are equally viable.

To explore the singlet states of these systems, their NMR properties must first be analyzed. The *Type-1* substrate, **1**, of

Table 1. ^{13}C (red/white dots) SABRE signal enhancement (ϵ) over the corresponding thermal measurement at 9.4 T after transfer at the indicated field (G), net polarization (P) and T_1 and T_2 lifetimes (s) of substrate **1–8** in high field (HF: 9.4 T) and low field (LF: ≈ 10 mT). The J -coupling between the ^{13}C spin-pair was found to be about 58.5 ± 2.0 Hz in all cases. The ΔJ_{CH} values for *Type-1* substrates, and the chemical shift difference ($\Delta\nu$) for *Type-2* substrates are noted.

Agent	Substrate structure	Enhancement (ϵ), Lifetime transfer field, net polarization level P [%]	Lifetime [s]	ΔJ_{CH}^* or $\Delta\nu@9.4$ T [Hz]
1		ϵ : 2500 ± 300 @30 G $P \approx 2.0$	T_1 : 9.7 ± 0.3 $T_{S(\text{HF})}$: 75 ± 5.5 $T_{S(\text{LF})}$: 115 ± 12	$3.1 \pm 0.2^*$
2		ϵ : 1600 ± 280 @150 G $P \approx 1.3$	T_1 : 12.4 ± 0.9 $T_{S(\text{HF/LF})}$: –	$^2J_{\text{CD}} \approx 0.4^*$
3		ϵ : 600 ± 50 @20 mG $P \approx 0.5$	T_1 : 16.0 ± 1.5 $T_{S(\text{HF/LF})}$: No access	0
4		ϵ : 1600 ± 300 @150 G $P \approx 1.3$	T_1 : 10.2 ± 0.6 $T_{S(\text{HF})}$: 22 ± 3.0 $T_{S(\text{LF})}$: 28 ± 6.5	11.0 ± 0.1
5		ϵ : 550 ± 50 @5 mG $P \approx 0.45$	T_1 : 15.5 ± 1.2 $T_{S(\text{HF})}$: 90 ± 3.0 $T_{S(\text{LF})}$: 165 ± 18	10.4 ± 0.1
6		ϵ : 350 ± 40 @10 mG $P \approx 0.35$	T_1 : 10.4 ± 0.3 $T_{S(\text{HF})}$: 115 ± 5.5 $T_{S(\text{LF})}$: 148 ± 20	14.5 ± 0.4
7		ϵ : 600 ± 50 @1 mG $P \approx 0.50$	T_1 : 15.2 ± 0.3 $T_{S(\text{HF})}$: 145 ± 6.0 $T_{S(\text{LF})}$: 186 ± 18	4.4 ± 0.3
8		ϵ : 800 ± 150 @10 mG $P \approx 0.65$	T_1 : 7.5 ± 0.5 $T_{S(\text{HF})}$: < 5 $T_{S(\text{LF})}$: 45 ± 6.0	78.8 ± 0.5

Table 1 reflects an AA'XX'-type spin system (Figure 1a) and produces the ^{13}C NMR spectrum shown in Figure 1b. This trace illustrates the effect of magnetic inequivalence, but does not immediately yield the individual carbon–proton couplings ($^2J_{\text{CH}}$ and $^3J_{\text{CH}}$) necessary to create a singlet state by the method of Warren,^[21] because the peak-to-peak separations reflect the mean value of the ^{13}C - ^1H J -couplings ($5.25 \text{ Hz} = [^2J_{\text{CH}} + ^3J_{\text{CH}}]/2$). By employing a J -synchronized experiment,^[23,30,32] it is possible to show that the difference in these J -couplings is 3.1 Hz (see Section S5 in the Supporting Information). We harness this difference in coupling (ΔJ_{CH}) to populate the singlet state through *rf* pulse-sequencing, as detailed in Figure 1c. Table 1 details the chemical structures of *Type-1* agents **1–3** that are examined here. A value of zero for ΔJ_{CH} means that it is not possible to induce interconversion between the singlet and triplets forms through *rf* pulsing (e.g., agent **3**, see Section S5).^[20]

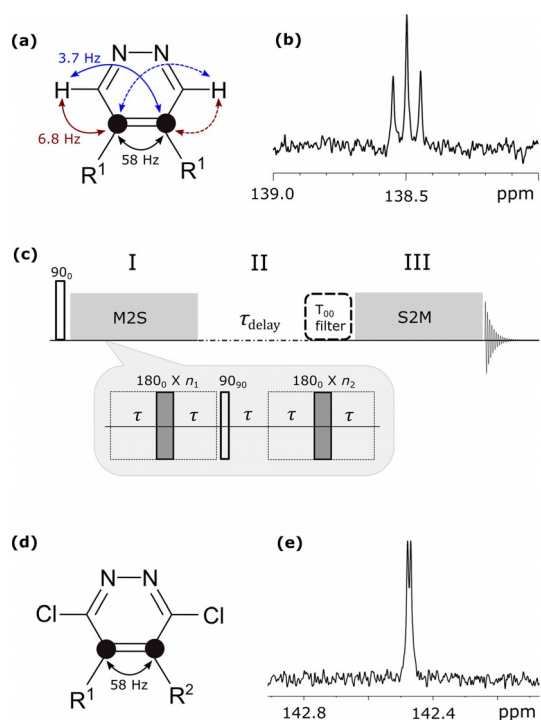


Figure 1. (a) Spin topology of the *Type-1* agent **1**, showing the J -couplings that exist between the ^1H and ^{13}C nuclei, in which R^1 = deuterated phenyl group; (b) corresponding ^{13}C NMR spectrum of agent **1** in $[\text{D}_4]\text{MeOH}$; (c) M2S-S2M pulse sequence used here; (d) spin topology of *Type-2* substrate **5** and corresponding ^{13}C NMR spectrum in $[\text{D}_4]\text{MeOH}$ (e).

We also prepared agents **4–8**, which reflect a series of *Type-2* molecular systems. Their spin system is illustrated in Figure 1d, whereas Figure 1e shows the ^{13}C NMR spectrum of agent **5** in $[\text{D}_4]\text{MeOH}$. In this case, the partially resolved 1.05 Hz ($\Delta\delta^2v^2/2J_{\text{CC}}$) splitting signifies that a strongly coupled ^{13}C spin-pair results when R^1 and R^2 are deuterated phenyl and *para*-tolyl groups, respectively.

The pulse sequence that is used to create and examine the lifetime of the singlet state in these *Type-1* and *-2* molecules consists of three parts, as detailed in Figure 1c. Part I converts longitudinal magnetization into singlet order (M2S), part II preserves this singlet order, and part III converts it back into a visible form. The first and last steps are realized experimentally by a train of n 180° pulses that are separated by delay (τ), which is a molecule-specific parameter. For the *Type-1* system, **1** in which $J_{\text{CC}} \gg J_{\text{HH}}$, Equations (1)–(3) provide τ and n .^[30,32]

$$\tau = \frac{1}{(2\sqrt{(J_{\text{CC}} + J_{\text{HH}})^2 + (\Delta J_{\text{CH}})^2})} \quad (1)$$

$$n_1 = \frac{\pi}{(2\tan^{-1}[\Delta J_{\text{CH}}/(J_{\text{CC}} + J_{\text{HH}})])} \quad (2)$$

$$n_2 \simeq n_1/2 \quad (3)$$

In contrast, in the case of the *Type-2* spin systems (agents **4–8**), these parameters come from Equations (3)–(5) shown above and below.

$$\tau = \frac{1}{(4\sqrt{J^2 + \Delta\delta^2v^2})} \quad (4)$$

$$n_1 = \frac{\pi}{(2\tan^{-1}[\Delta\delta \cdot v/J])} \quad (5)$$

Section S7 in the Supporting Information details these values for **1–8**. The resulting singlet states were then stored either in high field or in low field (after sample transfer). For **1**, the singlet state lifetimes (T_S) were measured to be 75 ± 5.5 and 115 ± 12 s at high and low field, respectively. We therefore see about a 10-fold increase over the 9.4 T T_1 relaxation time of 9.7 s. The effect of a spin-lock during high-field storage proved to be minimal, increasing the T_S by only about 10%. In the case of agent **5**, we achieved a T_S of 90 ± 3 s in high field, which increases to 165 ± 18 s in low-field. Table 1 summarizes these values for agents **1–8** and confirms that this strategy allows the creation of long-lived singlet states in these molecules. ^2H -labeled **7** contained the optimal molecular environment of the series, delivering a low-field T_S of 186 ± 18 s.

For **2**, the ^{13}C - ^2H couplings are too small to exploit the M2S sequence to prepare the singlet. For **4**, the singlet-state lifetime proved low due to the ^{13}C -deuterium coupling, which provides a route to scalar relaxation.^[35] In **8**, the chemical shift difference between the ^{13}C pairs is similar to the J -coupling constant in high field and a low lifetime results but in low field this extends to 45 s. In contrast, agents **5**, **6** and **7** operate well in both low and high field, exhibiting lifetimes in excess of 150 s in low field.

A series of SABRE experiments were then undertaken to see if it was possible to create hyperpolarized longitudinal spin order within the ^{13}C manifold of agents **1–8** (Table 1). This involved taking $[\text{D}_4]\text{MeOH}$ solutions that contained 20 mM of the substrate, and 5 mM of the IMes catalyst. $p\text{-H}_2$ gas was bubbled through the solution for 20 s in low field and the sample transferred into the NMR spectrometer for further analysis. Figure 2 highlights the results of this process, with the level of ^{13}C polarization reaching about 2% as compared to the corresponding thermal polarization of only 0.0008% at 9.4 T in the

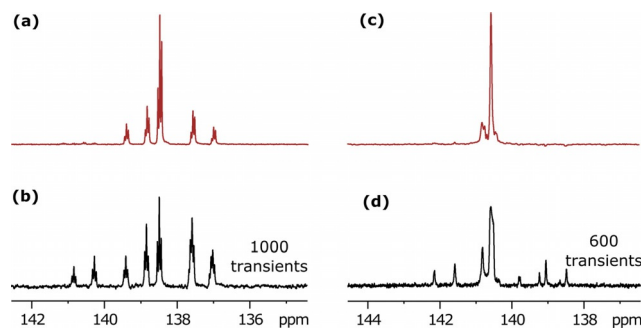


Figure 2. ^{13}C NMR spectra of **1** after (a) SABRE at a mixing field 5 mG and corresponding thermally equilibrated signal of 1000 transients. (c) Similar SABRE studies of **7** at a mixing field of 1 mG and (d) its thermal equilibrium spectra acquired by 600 transients.

case of agent **1** after relayed transfer from ^1H - ^{13}C at 30 G (see Section S6 in the Supporting Information). No H/D-exchange is observable on the timescale of the SABRE experiment. The relayed transfer process was then examined as a function of the magnetic field experienced by the sample, and three maxima were observed, at about 10 mG (using μ -metal shield), 30 and 100 G. Simulation revealed the about 10 mG maxima is associated with direct hydride-carbon spin-spin transfer by the $^4J_{\text{H}-^{13}\text{C}}$ and $^5J_{\text{H}-^{13}\text{C}}$ couplings in the catalyst. The remaining maxima appear to result from relayed transfer by the agents ^1H response (see Section S4).

When agent **2** is examined, the ^2H labels should prevent the relayed response that is operating and restrict its transfer to the approximate 10 mG field range. Under these conditions, a strong ^{13}C signal is seen. However, upon moving from 10–150 G, ^{13}C and ^1H SABRE enhanced signals are observed in the ^1H and ^{13}C frequency ranges. These results reveal readily detectable contributions from the ^2H - ^1H isotopologue, which is present at 1%, through the observation of a ^{13}C response that contains a $J_{\text{H}-^{13}\text{C}}$ splitting of 5.4 Hz. This reflects one of the challenges faced when working with hyperpolarization in so far as low-concentration species can be readily detected. Agents **3** and **5–8** also require direct polarization transfer because there is no suitable relayed transfer pathway and they once again work well between 1 and 20 mG. These ^{13}C hyperpolarization data are summarized in Table 1 (and Section S5). Polarization levels approaching 2% are readily achieved, which would be expected to increase further through catalyst optimization.^[36] We then transferred the resulting ^{13}C -hyperpolarization into singlet order using the methods described earlier. The efficiency of singlet conversion in all successful cases was found to be in the range of 50–80%.

Figure 3 shows the decay of the resulting hyperpolarized ^{13}C singlet derived signals for agents **1**, **5–8** as a function of their storage time (T_s) in low field. The ^{13}C lifetimes proved to be directly comparable to those measured without hyperpolarization and signals can be readily observed for several minutes after creation when stored in a low-field region. In the case of **7**, hyperpolarized signals were detectable for well over 10 mins.

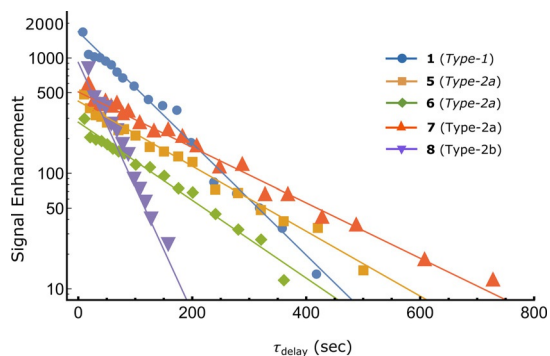


Figure 3. Hyperpolarized ^{13}C singlet state decay (log10 scale) as a function of low-field storage time (τ_{delay}) for agents **1**, **5–8**. Results are summarized in Table 1.

In summary, we have demonstrated that a series of novel agents can be prepared that contain two adjacent ^{13}C labels in addition to two nitrogen-based lone pairs, which make them suitable for SABRE. Despite the weak J -coupling that exists between the hydride ligands and the targeted ^{13}C sites, we achieve a hyperpolarized response at the 2% level. This hyperpolarization has then been efficiently converted into singlet spin order within the two ^{13}C labels by rf excitation with a low-field relaxation time of about 190 s being the result for deuterated dimethyl *p*-tolyl phenyl pyridazine. This process has been exemplified for both magnetic and chemical inequivalence. Our method provides a fast and low-cost technique to create ^{13}C hyperpolarization in a reversible fashion with very little waste. Because of the simplicity of this approach, we envisage that this strategy will be adopted more widely to hyperpolarize related tracers. We are currently seeking to improve on the purity of these states to test the in vivo detection of these agents.

Acknowledgements

We thank the Wellcome Trust (092506 and 098335) for funding. We are grateful to discussions with Prof. H. Perry. Supporting information via: DOI: 10.151244a012088-7b46-4dcb-96eb-a1a78e8ffa96.

Conflict of interest

The authors declare no conflict of interest.

Keywords: hyperpolarization · long-lived singlet states · NMR spectroscopy · *para*-hydrogen · structure elucidation

- [1] J. H. Lee, Y. Okuno, S. Cavagnero, *J. Magn. Reson.* **2014**, *241*, 18–31.
- [2] J.-H. Ardenkjaer-Larsen, *Angew. Chem. Int. Ed.* **2015**, *54*, 9162–9185; *Angew. Chem.* **2015**, *127*, 9292–9317.
- [3] J. Natterer, J. Bargon, *Prog. Nucl. Magn. Reson. Spectrosc.* **1997**, *31*, 293–315.
- [4] C. R. Bowers, D. P. Weitekamp, *Phys. Rev. Lett.* **1986**, *57*, 2645–2648.
- [5] K. Golman, O. Axelsson, H. Johannesson, S. Mansson, C. Olofsson, J. S. Petersson, *Magn. Reson. Med.* **2001**, *46*, 1–5.
- [6] K. Golman, J. H. Ardenaer-Larsen, J. S. Petersson, S. Mansson, I. Leunbach, *Proc. Natl. Acad. Sci. USA* **2003**, *100*, 10435–10439.
- [7] P. Bhattacharya, E. Y. Chekmenev, W. H. Perman, K. C. Harris, A. P. Lin, V. A. Norton, C. T. Tan, B. D. Ross, D. P. Weitekamp, *J. Magn. Reson.* **2007**, *186*, 150–155.
- [8] S. J. Nelson, *Science Translational Medicine* **2013**, *5*.
- [9] K. Golman, R. in't Zandt, M. Lerche, R. Pehrson, J. H. Ardenkjaer-Larsen, *Cancer Res.* **2006**, *66*, 10855–10860.
- [10] K. Golman, R. in't Zandt, M. Thaning, *Proc. Natl. Acad. Sci. USA* **2006**, *103*, 11270–11275.
- [11] S. E. Day, M. I. Kettunen, F. A. Gallagher, D.-E. Hu, M. Lerche, J. Wolber, K. Golman, J. H. Ardenkjaer-Larsen, K. M. Brindle, *Nat. Med.* **2007**, *13*, 1382–1387.
- [12] R. W. Adams, J. A. Aguilar, K. D. Atkinson, M. J. Cowley, P. I. P. Elliott, S. B. Duckett, G. G. R. Green, I. G. Khazal, J. Lopez-Serrano, D. C. Williamson, *Science* **2009**, *323*, 1708–1711.
- [13] N. Eshuis, B. J. A. van Weerdenburg, M. C. Feiters, F. P. J. T. Rutjes, S. S. Wijmenga, M. Tessari, *Angew. Chem. Int. Ed.* **2015**, *54*, 1481–1484; *Angew. Chem.* **2015**, *127*, 1501–1504.

- [14] A. N. Pravdivtsev, A. V. Yurkovskaya, H.-M. Vieth, K. L. Ivanov, *J. Phys. Chem. B* **2015**, *119*, 13619–13629.
- [15] G. Heinisch, H. Frank, *Prog Med Chem.* **1990**, *27*, 1–49.
- [16] M. Asif, *Curr. Med. Chem.* **2012**, *19*, 2984–2991.
- [17] S. S. Roy, P. J. Rayner, P. Norcott, G. G. R. Green, S. B. Duckett, *Phys. Chem. Chem. Phys.* **2016**, *18*, 24905–24911.
- [18] S. S. Roy, P. Norcott, P. J. Rayner, G. G. Green, S. B. Duckett, *Angew. Chem. Int. Ed.* **2016**, *55*, 15642–15645; *Angew. Chem.* **2016**, *128*, 15871–15874.
- [19] T. Theis, *Sci. Adv.* **2016**, *2*, e1501438.
- [20] M. H. Levitt, in *Annu. Rev. Phys. Chem., Vol. 63* (Eds.: M. A. Johnson, T. J. Martinez), **2012**, pp. 89–105.
- [21] W. S. Warren, E. Jenista, R. T. Branca, X. Chen, *Science* **2009**, *323*, 1711–1714.
- [22] M. Carravetta, M. H. Levitt, *J. Am. Chem. Soc.* **2004**, *126*, 6228–6229.
- [23] M. C. D. Tayler, M. H. Levitt, *Phys. Chem. Chem. Phys.* **2011**, *13*, 5556–5560.
- [24] M. C. D. Tayler, I. Marco-Rius, M. I. Kettunen, K. M. Brindle, M. H. Levitt, G. Pileio, *J. Am. Chem. Soc.* **2012**, *134*, 7668–7671.
- [25] G. Pileio, J. T. Hill-Cousins, S. Mitchell, I. Kuprov, L. J. Brown, R. C. D. Brown, M. H. Levitt, *J. Am. Chem. Soc.* **2012**, *134*, 17494–17497.
- [26] G. Stevanato, S. S. Roy, J. Hill-Cousins, I. Kuprov, L. J. Brown, R. C. D. Brown, G. Pileio, M. H. Levitt, *Phys. Chem. Chem. Phys.* **2015**, *17*, 5913–5922.
- [27] G. Stevanato, J. T. Hill-Cousins, P. Hakansson, S. S. Roy, L. J. Brown, R. C. D. Brown, G. Pileio, M. H. Levitt, *Angew. Chem. Int. Ed.* **2015**, *54*, 3740–3743; *Angew. Chem.* **2015**, *127*, 3811–3814.
- [28] G. Pileio, M. Carravetta, M. H. Levitt, *Proc. Natl. Acad. Sci. USA* **2010**, *107*, 17135–17139.
- [29] Y. Zhang, P. C. Soon, A. Jerschow, J. W. Canary, *Angew. Chem. Int. Ed.* **2014**, *53*, 3396–3399; *Angew. Chem.* **2014**, *126*, 3464–3467.
- [30] Y. Feng, T. Theis, T.-L. Wu, K. Claytor, W. S. Warren, *J. Chem. Phys.* **2014**, *141*, 134307.
- [31] K. Claytor, T. Theis, Y. Feng, W. Warren, *J. Magn. Reson.* **2014**, *239*, 81–86.
- [32] Y. Feng, R. M. Davis, W. S. Warren, *Nat. Phys.* **2012**, *8*, 831–837.
- [33] J. F. P. Colell, *J. Phys. Chem. C* **2017**, *121*, 6626–6634.
- [34] J.-B. Hövener, *Anal. Chem.* **2014**, *86*, 1767–1774.
- [35] G. Pileio, *Prog. Nucl. Magn. Reson. Spectrosc.* **2010**, *56*, 217–231.
- [36] P. J. Rayner, M. J. Burns, A. M. Olaru, P. Norcott, M. Fekete, G. G. R. Green, L. A. R. Highton, R. E. Mewis, S. B. Duckett, *Proc. Natl. Acad. Sci. USA* **2017**, *114*, E3188–E3194.

Manuscript received: June 16, 2017

Accepted manuscript online: June 19, 2017

Version of record online: July 19, 2017